

Research Paper**REE AND GALLIUM IN THE DIASPORITE DEPOSITS OF MIKRI LAKKA, EAST SAMOS ISLAND, GREECE****Michael G. Stamatakis^{1*} and Alexandra Koltiri²**¹*NKUA, Department of Geology and Geoenvironment, Panepistimiopolis Ano**Ilissia 157 84, Athens, Greece, stamatakis@geol.uoa.gr*²*Corinth Pipeworks SA, Thisvi Boeotia Industrial Area, Greece*akoltiri@cpw.vionet.gr**corresponding author***Abstract**

In Samos Island, Aegean Sea, Greece, several diasporite and emery occurrences and idle mines occur. The major diasporite deposit is developed at the eastern part of the island at Mourtia, Mikri Lakka where there exist old mining works. The specific metabauxite is hosted, via a transition zone, in between marble of Mesozoic age which has been tectonically disturbed. The aim of the present study is to characterize the metabauxite deposit and to investigate its content in specific trace elements and especially REE and gallium. XRD, XRF and SEM-EDS analysis carried out in representative samples of the massive diasporite deposit, the transition zone and the associated marble. XRD analysis revealed that the marble is calcitic. The transition zone is mainly composed of muscovite, illite, kaolinite, quartz and calcite with minor amounts of diasporite, whereas the main ore body is composed mainly of diasporite, followed by minor-trace amounts of calcite, muscovite, magnetite, hematite and quartz. XRF major element analysis has shown that the ore body is rich in alumina and secondarily in iron oxides. The trace element analysis discloses a notable enrichment in Ga, some REE and zirconium. Gallium is not detected by SEM-EDS as any gallium mineral, and it is most likely being fixed in the lattice of diasporite. It is concluded that the derivation of all trace elements enrichments and the source of alumina from the Mesozoic rocks of the Ampelos Nape, which included originally sedimentary rocks, gabbro and volcanics. These rocks were weathered and altered under wet conditions releasing silica, alumina and iron, which formed bauxite deposits rest on a limestone

Correspondence to:
Michael G. Stamatakis
stamatakis@geol.uoa.gr

DOI number:
<http://dx.doi.org/10.12681/bgsg.40816>

Keywords: Metabauxite; diasporite; gallium; REE; Samos Island.

Citation:
Stamatakis, M.G., and Koltiri, A. 2025. REE and Gallium in the diasporite deposits of Mikri Lakka, east Samos Island, Greece. Bulletin Geological Society of Greece, 62, 1-28.

Publication History:
Received: 17/03/2025
Accepted: 12/06/2025
Accepted article online: 29/07/2025

The Editor wishes to thank the reviewers for their work with the scientific reviewing of the manuscript, Dr Sotirios Valkaniotis for his help with Fig. 1 and Mr Georgios Goutsos for editorial assistance.

©2025. The Authors
This is an open access article under the terms of the Creative Commons Attribution License, which permits use, distribution and reproduction in any medium, provided the original work is properly cited.

substrate. Finally, the limestone-bauxite succession was metamorphosed and tectonically disturbed. Concerning the economic importance of the Mikri Lakka diasporite, it is noted that bauxite/diasporite deposits have a potential of hosting significant REE concentrations. The average gallium content of the Mikri Lakka massive diasporite is 79 ppm (max of 96 ppm), which is higher than the average gallium content of the bauxite deposits and occurrences of Parnassus-Ghiona-Oiti Greece. Both the REE and gallium content of the Mikri Lakka diasporite is promising to consider their recovery as byproducts during diasporite exploitation, despite the fact that its proven reserves in the east part of Samos are unknown.

Keywords: Metabauxite, diasporite, gallium, REE, Samos Island

ΠΕΡΙΛΗΨΗ

Στη νήσο Σάμο, Αιγαίο Πέλαγος, Ελλάς, έχουν εντοπισθεί μερικά ανενεργά μεταλλεία και εμφανίσεις σμύριδας και διασπορίτη. Η κύρια απόθεση διασπορίτη συναντάται στην ανατολική Σάμο, στη θέση Μουρτιά – Μικρή Λάκκα, όπου υπάρχουν παλαιά μεταλλευτικά έργα. Ο συγκεκριμένος διασπορίτης είναι ένας μεταβωξίτης που αναπτύσσεται, μέσω μιας μεταβατικής ζώνης, μεταξύ τεκτονικά καταπονημένων μαρμάρων Μεσοζωικής ηλικίας. Καθώς ο μεταβωξίτης προέρχεται από ένα βωξιτικό μητρικό υλικό, αναμένεται να περιέχει αυξημένες συγκεντρώσεις συγκεκριμένων μεταλλικών ιχνοστοιχείων. Σκοπός της παρούσης εργασίας είναι ο χαρακτηρισμός της μεταβωξιτικής απόθεσης και ο προσδιορισμός της περιεκτικότητας μεταλλικών ιχνοστοιχείων και ειδικά του γαλλίου και των σπανίων γαιών. Για τους σκοπούς αυτούς χρησιμοποιήθηκαν αναλυτικές μέθοδοι όπως XRD, XRF και SEM-EDS σε μια σειρά αντιπροσωπευτικών δειγμάτων συμπαγούς διασπορίτη, γεώδους μεταβατικής ζώνης και μαρμάρου. Η ορυκτολογική (XRD) ανάλυση έδειξε ότι τα μάρμαρα είναι ασβεστιτικά, η γεώδης μεταβατική ζώνη αποτελείται κυρίως από τα ορυκτά μοσχοβίτης, ιλλίτης, καολινίτης, χαλαζίας και ασβεστίτης, ενώ περιέχονται και μικρά ποσά διασπόρου, ενώ ο συμπαγής διασπορίτης αποτελείται κυρίως από διάσπορο το οποίο συνοδεύεται από κυμαινόμενα αλλά μικρά ποσά ασβεστίτη, μοσχοβίτη, μαγνητίτη, αιματίτη και χαλαζία. Η χημική (XRF) ανάλυση κύριων στοιχείων και ιχνοστοιχείων έδειξε ότι ο συμπαγής διασπορίτης αποτελείται κυρίως από Al_2O_3 και δευτερογενώς από σιδηροξείδια. Η ανάλυση ιχνοστοιχείων έδωσε αξιοσημείωτους εμπλουτισμούς σε Ga, REE και Zr. Ο συμπαγής διασπορίτης περιέχει υψηλότερα ποσά Sc, V, Cr, Ga, Y, Nd, Sm και Ce, ενώ η γεώδης μεταβατική ζώνη περιέχει υψηλότερα ποσά As, Ba, S, Cu, Zn, Pb, and Mo. Γενικά οι υψηλές τιμές Ga ακολουθούν την αύξηση περιεκτικότητας Al_2O_3 στα δείγματα, όπως επίσης και τις περιεκτικότητες Zr, το οποίο συναντάται με τη μορφή $ZrSiO_4$, καθώς γνωστές δευτερογενείς ορυκτολογικές φάσεις απουσιάζουν. Στα διαγράμματα Pearsons, η σχέση Ga- Al_2O_3 φθάνει το 0.9851, η σχέση Ga-Zr 0.8639 και η σχέση Zr- Al_2O_3 0.8904. Κατά την ανάλυση SEM-EDS, τα στοιχεία των σπανίων γαιών Ce, Y, Nd, La, Hf, Sm, Pr, Gd, Er, εντοπίστηκαν με τη μορφή κλαστικών κόκκων βυθισμένων μέσα σε μια κύρια μάζα πλούσια σε αργίλιο. Οι κόκκοι αυτοί είναι είτε πλούσιοι σε P_2O_5 , συνθέτοντας μοναζίτες με κυμαινόμενη σύσταση, ή δε σχετίζονται καθόλου με φώσφορο, σχηματίζοντας άλλα ορυκτά των σπανίων γαιών. Το Ga δεν εντοπίστηκε ως αυτοτελές

ορυκτό του γαλλίου κατά την ανάλυση SEM-EDS, και πιθανότατα είναι ενσωματωμένο στο κρυσταλλικό πλέγμα του διασπόρου. Συμπεραίνεται ότι η προέλευση των εμπλουτισμών των ιχνοστοιχείων και η πηγή του αργιλίου είναι από τα Μεσοζωικά πετρώματα του τεκτονικού καλύμματος της Αμπέλου, το οποίο αρχικά αποτελείτο από ιζηματογενή πετρώματα, γάββρο και ηφαιστίτες. Αυτά τα πετρώματα αποσπάρθηκαν και εξαλλοιώθηκαν σε υγρές συνθήκες, ελευθερώνοντας Al, Fe, Si, τα οποία σχημάτισαν βωξιτικές αποθέσεις πάνω σε ένα ασβεστολιθικό υπόβαθρο. Τελικά, η ακολουθία ασβεστόλιθων-βωξίτη υπέστη μεταμορφικές διεργασίες και καταπονήθηκε τεκτονικά. Όσον αφορά την οικονομική σημασία των αποθέσεων διασπορίτη της Μικρής Λάκκας, σημειώνεται ότι σε συσχετισμό με βωξιτικά κοιτάσματα, έχουν ένα δυνητικό να φιλοξενούν σημαντικές συγκεντρώσεις σπανίων γαιών. Η μέση περιεκτικότητα γαλλίου του συμπαγούς διασπορίτη της Μικρής Λάκκας είναι 79 ppm (μέγιστη περιεκτικότητα 96 ppm), η οποία είναι υψηλότερη από τη μέση περιεκτικότητα γαλλίου των βωξιτικών κοιτασμάτων και εμφανίσεων των περιοχών Παρνασσού-Γκιώνας-Οίτης. Οι περιεκτικότητες σε REE και Ga του διασπορίτη της Μικρής Λάκκας είναι ευνοϊκές για την απόληψη αυτών ως παραπροϊόντων κατά την εκμετάλλευση του διασπορίτη, παρά το γεγονός ότι τα βέβαια αποθέματά του στην ανατολικά Σάμο είναι άγνωστα.

Λέξεις – Κλειδιά: μεταβωξίτης, διασπορίτης, γάλλιο, σπάνιες γαίες, νήσος Σάμος

1. Introduction

Emery deposits in the Aegean Archipelago are widespread on the island of Naxos and less in the islands of Samos, Ikaria, Ios, Sikinos and Herakleia. According to the most dominant theory, emery is characterized as metabauxite, due to its origin through the process of metamorphism of bauxites (Urai and Feenstra, 2001; Feenstra et al. 2001). In the Aegean Region, this metamorphism has taken place during the Alpine orogenesis under specific conditions of pressure and temperature (Löwen et al. 2015). In general, metabauxites are classified into two general categories, according to the principal constituent elements they contain: diasporite, which is rich in diasporite $\text{AlO}(\text{OH})$, and emery, which is rich in corundum Al_2O_3 , the mineral that gives emery its great hardness and abrading attributes. The second type of metabauxites has been formed after the dehydration of diasporite; they are, therefore, metabauxites of a higher degree of metamorphism (Boleti 2014; Feenstra 1985; Urai and Feenstra 2001).

In Samos Island, several diasporite and emery occurrences and idle mines occur (Dimou et al. 2006; Stamatakis and Malegiannaki, 2018). In the east part of the island (Figure 1) at Mourtia, Mikri Lakka, metabauxite deposits of diasporite type occur, which were exploited during the 1930's. The specific diasporites are hosted in between Mesozoic marbles of the Ampelos Nappe which have been tectonically disturbed. The estimated P-T conditions of the metamorphic event in Ampelos Nappe are ranging from 420-490°C and 6-15 kbar (Ring et al. 1999; Ring et al. 2007).

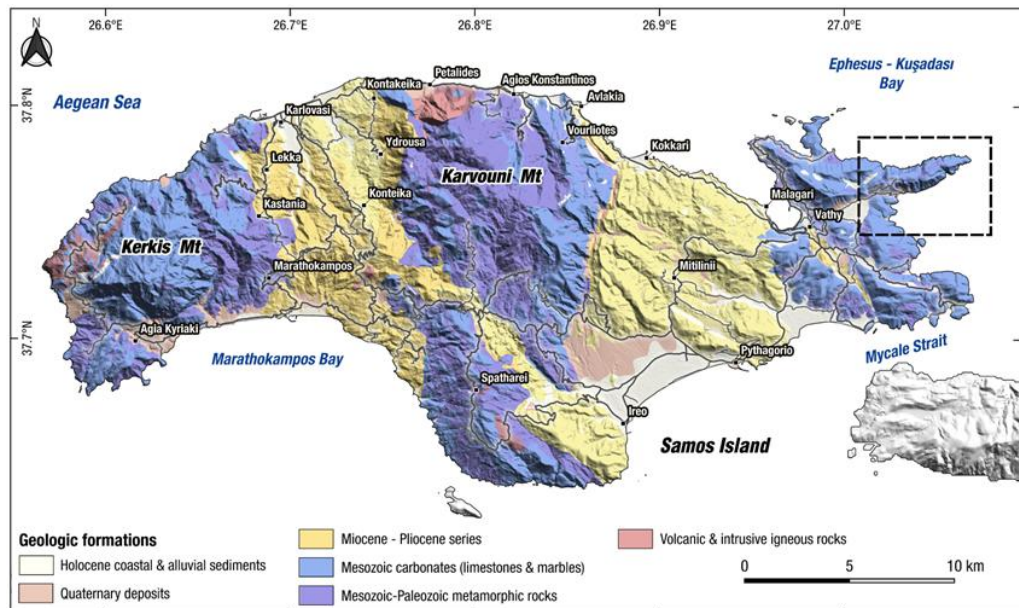


Fig. 1: The Pre-Neogene basement rocks and the Late Neogene sedimentary rocks of Samos Island (modified after Ganas et al. 2021). The dashed rectangular outlines the studied area.

As meabauxites are metamorphosed bauxitic deposits, there generally exists the possibility to be similarly rich in specific trace elements, Ga and REE among them. Lateritic bauxites, formed during alteration of several types of parent rocks, therefore, the composition of the bauxite source rock plays the most important role in the distribution of major and trace elements in each particular deposit. The parent rocks are being either anorthositic, argillite and dolerite, granulite and feldspathic gneiss, and/or mafic-basaltic andesite (Zainudeen et al. 2023). Iron content and mineralogy of the bauxite affect distribution of trace elements in it, as well as the chemical characteristics of the elements which were transferred into the basin as stable, weakly soluble (Zr, Ga) and mobile phases, along with aluminum (Mordberg 1993). The variance in major and trace element content of the bauxites is affected by factors such as stability of host minerals, fixation of elements in authigenic phases, preferential sorption, and the pH of percolating waters (Calagari and Abedini, 2007).

Gallium is rarely forming individual gallium minerals, but it is found in trace amounts within minerals, substituting elements with similar sizes and charges, such as zinc or aluminum (Rudnik 2024). As a result, gallium is commercially extracted from bauxite and zinc ores (Foley et al 2017; USGS 2021). The aluminum-bearing minerals of bauxites diaspore $\gamma\text{-AlOOH}$, boehmite $\alpha\text{-AlOOH}$ and gibbsite $\text{Al}(\text{OH})_3$, may host variable Ga concentrations (Schulte and Foley 2014; Qi et al 2023; Rudnik 2024).

Recently, high grade gallium mineralization reaching 232 ppm Ga was discovered in fluorite deposits which are also rich in REE (Zemeyi, 2025).

Concerning the distribution of REE in bauxites, Villanova et al. (2023) describe, karstic bauxite deposits located in the Dominican Republic which are ultra-rich in REE. In a geo-archaeological paper on the Mikri Lakka diasporite deposit of Samos, monazite rich in Ce, La and Nd has been detected (Stamatakis and Malegiannaki, 2018). The aim of the present study is to characterize the metabauxite deposit of Mikri Lakka and to investigate its content in specific trace elements and especially REE and gallium.

2. Geological Setting of Eastern Samos

The island of Samos is located in the eastern Aegean Sea near the coast of Western Anatolia. Pre-Neogene rocks are composed of marble, dolomite, quartz, shale, hornfelse, and igneous rocks (Ring et al., 1999, 2007). The metamorphic rocks of the island belong to the tectonic units of Kerketeas, South and Northern Cyclades (Papanikolaou, 1979 and 2021) and were developed under a tectonic extension system trending N-S. On this pre-Neogene basement, two main basins were developed, the Mytilinii basin to the east and the Karlovassi basin to the west. The deposits of the two basins are interpreted as of continental character, of Upper Miocene age (Bessenecker and Buttner, 1978; Theodoropoulos, 1979a&b; Weidman et al. 1984; Stamatakis 1986).

In east Samos, close to the seashore at Mikri Lakka (Figure 1), four mine tunnels occur in parallel penetrating the Cretaceous marble, as well as traces of Decauville railroad that was used for the transportation of the ore from the mines to the shore. Southwards, at the seashore which is 240 m far from the entrance of the underground mines, a quantity of some 1000 tons of diasporite remains stockpiled. Besides Mikri Lakka, metabauxite deposits are also found southwest of Vathy, and in west Samos at the site of Kalabachtasi (Lapparent 1937; Mposkos 1986). These deposits are dispersed and form lenses hosted in Cretaceous marbles which contain rudists (Papanikolaou, 1979) of the Ampelos Unit (Gessner et al., 2011). Based on old reports, the reserves of the diasporite deposits in Mikri Lakka are estimated up to ~ 35,000 tons (Dimou et al., 2006). After Ring et al. (1999), the Mesozoic rocks in the studied area belong to Ampelos nappe. Tectonically, Mikri Lakka marbles/diasporite succession is disturbed, forming a recumbent anticline (Figure 2), (Papanikolaou 1979); hence the diasporite deposit is sandwiched in between Upper Cretaceous marble that contain relics of rudists (Figure 3).



Fig. 2: The tectonically disturbed succession of Mikri Lakka. The ribbon bluish gray-white marble and relics of reddish metabauxite forming a recumbent anticline of E-W direction (uppermost left). The bluish grey marble lies on the yellowish-brown transitional fluffy deposits, whereas purple diasporite is situated at the bottom of the outcrop (uppermost right). The sharp contact of the yellowish transition deposits with the massive reddish-purple diasporite (lowermost left). Massive diasporite masses which show well developed three-dimensional system of joints (lowermost right).

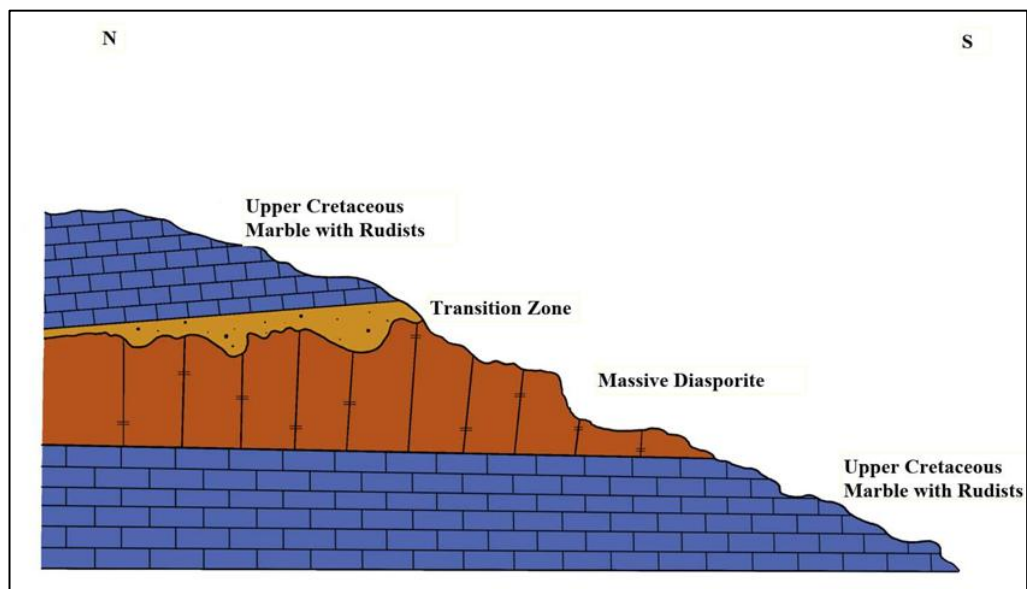


Fig. 3: Schematic cross-section of the folded (recumbent anticline) metamorphic succession in Mikri Lakka.

The tectonically upper contact of the diasporite with the marble is characterized as transition zone having a feature of an inhomogeneous flaky-earthy deposit (Figure 2). By contrast, the main body of the metabauxite even fractured, is massive, whereas a

well-developed three-dimensional system of joints yield long prismatic pieces of ore, sometimes filled by secondary calcite (Figure 2).

3. Materials and Methods

Twelve samples were collected from the two main parallel shallow (<15 m) galleries, located at 37°45'32.46"N and 27°1'21.20"E, running into metabauxite which are developed in a mine-face of 100 m, and one sample from the overlying marble (SML-MR). The samples extracted from the galleries were divided to those taken from the metallic grey massive ore (SML-DS), and the earthy brownish-yellow deposit of the transition zone (SML-BS) which is developed on the contact of the marble with the ore. The samples were dried, crushed and partially pulverized at TITAN R&D laboratory of the Kamari-Boeotia Cement plant. The rock powder was used for XRD mineralogical and XRF chemical analysis, whereas chip samples were used for SEM-EDS analysis. XRD analysis was performed for identification of the bulk mineralogy of the samples at TITAN SA, Kamari Plant using the instrument X BRUKER D8 ADVANCED, in running conditions: 40kV, 40mA, 1o/min, Cu-Ka radiation. XRF analysis carried out for measuring of the major and trace elements chemistry of the samples at TITAN SA Kamari Plant, using the SRS 3400 wavelength dispersive XRF Spectrometer, Bruker form major elements, and the Epsilon 5 energy dispersive XRF Spectrometer Panalytical, for trace elements. SEM-EDS analysis was performed to identify the presence and nature of REE and other micro-constituents of the metabauxite at NKUA, Department of Geology and Geoenvironment, using the JEOL JSM-5600, combined with microanalyzer energy dispersive system OXFORD LINK ISIS 300, with software ZAF correction quantitative analysis. The system was operating at 20KV, 0.5nA and 50 sec time of analysis. The analytical results are presented in Tables 1 and 2 a&b, and Plates 1 and 2 (see Appendix section of the article).

4. Results and Discussion

XRD mineralogical analysis revealed that the marbles are calcitic, containing small amounts of dolomite, quartz and muscovite/illite, the fluffy transitional metabauxite deposit is mainly composed of muscovite, illite, kaolinite, quartz and calcite with minor amounts of diaspor, whereas the main ore body is composed mainly of diaspor, followed by minor amounts of calcite and muscovite (Table 1). Small to trace amounts of magnetite, hematite and quartz are also present. Corundum was not found in the samples studied, and the single-Al₂O₃ phase is represented by only diaspor. The

absence of corundum classifies the metabauxite deposits of Mikri Lakka as low to medium metamorphism deposits.

Table 1: XRD mineralogical analysis of the Cretaceous marble (MR), transition (BS), and massive diasporite deposit (DS) of Mikri Lakka.

Samples	Cc	Dol	Dsp	Qtz	Mc	Kaol	Ill	Hem	Mgn
SML-MR-1	MJ	TR		TR					
SML-BS-1	MJ		TR	TR	TR				
SML-BS-2	MJ		TR	TR	TR				
SML-BS-3	MD				MD		MD		
SML-BS-4	MD		TR		MJ				
SML-BS-5	MD		MJ	TR	MD	MD		TR	TR
SML-BS-6	MD				MD	MD		TR	TR
SML-DS-1			MJ		MD	MD		TR	TR
SML-DS-2			MJ		MJ			TR	TR
SML-DS-3-vein	MD			MD	MD			TR	TR
SML-DS-4			MJ			MD		TR	TR
SML-DS-5-vein	MD			MD	MJ			TR	TR
SML-DS-6			MJ		MJ	MD			

Explanatory notes:

Cc= calcite, Dol=dolomite, Dsp= diasporite, Qtz= quartz, Kaol=kaolinite, Mc=Muscovite, Ill= illite, Hem= Hematite, Mgn= Magnetite & Titanomagnetite. MJ=major, MD= medium, TR= trace/minor constituent. Amorphous Fe- and Fe/Mn-rich phases are also present.

The major and the trace element content of the samples reflect their mineralogical composition. The marble has as predominant oxide the CaO, whereas the diasporite has Al_2O_3 as predominant oxide, followed by Fe_2O_3 and SiO_2 (Table 2a & b). The transitional yellowish horizons (Figure 2) are characterized by a mixed-up composition varying between CaO-rich and Al_2O_3 - Fe_2O_3 - SiO_2 -rich samples (Table 2). Notably, the iron-rich samples have elevated content of TiO_2 which is attributed to the presence of titanomagnetite and secondarily to trace amounts of rutile and ilmenite crystals. The XRF trace element analysis discloses a notable enrichment in Ga, some REE and other elements (Table 2). The massive body of the metabauxite has higher values of Sc, V, Cr, Ga, Y, Nd, Sm and Ce, whereas the transition calcareous rock/diasporite deposit has higher values in As, Ba, S, Cu, Zn, Pb, and Mo. The elements Ni, Co, Rb, Ge, and Hf have almost equal high values in the metabauxite studied. In general, Ga high values are following the increase content of alumina in the samples, but also the high Zr values which are related with the presence of zircon.

Table 2: XRF chemical analysis of major elements (a) and trace elements (b) of the Cretaceous marble (MR), transition (BS), and massive diasporite deposit (DS) of Mikri Lakka.

Table 2a:

oxides	SML-MR-1	SML-BS-1	SML-BS-2	SML-BS-3	SML-BS-4	SML-BS-5	SML-BS-6	SML-DS-1	SML-DS-2	SML-DS-3	SML-DS-4	SML-DS-5	SML-DS-6
P ₂ O ₅ %	BDL	BDL	BDL	BDL	BDL	0.06	BDL	0.04	0.01	BDL	0.03	0.05	0.02
SO ₃ %	0.04	0.20	0.08	0.05	0.01	0.07	0.10	0.03	0.15	0.10	0.03	0.05	0.03
K ₂ O%	0.20	0.50	1.40	1.20	0.10	3.70	4.00	1.00	0.40	3.60	0.80	3.70	0.30
CaO%	48.13	43.00	39.20	39.00	43.00	17.80	11.00	0.90	4.30	5.90	1.00	3.00	2.50
TiO ₂ %	0.02	0.13	0.30	0.25	0.16	1.37	1.14	2.56	2.60	2.42	2.60	2.10	0.09
Fe ₂ O ₃ %	0.30	2.60	2.04	2.20	1.90	12.90	14.50	21.50	20.40	16.50	20.50	15.65	28.70
SiO ₂ %	1.20	9.00	14.00	13.00	7.80	28.00	32.50	9.00	17.40	24.00	18.40	33.60	29.00
Al ₂ O ₃ %	0.70	5.50	9.00	8.50	4.50	30.50	26.70	63.00	53.00	44.00	56.00	41.40	38.50
MnO%	BDL	0.10	0.02	0.03	0.10	0.30	2.00	0.03	0.20	0.03	0.08	0.10	0.20
MgO%	2.40	BDL	BDL	BDL	1.64	BDL	BDL	1.40	1.30	BDL	0.40	BDL	0.40
Na ₂ O%	BDL	BDL	BDL	BDL	BDL	BDL	BDL	BDL	BDL	BDL	BDL	BDL	BDL
LOI%	47.12	39.01	33.84	35.70	40.85	5.70	8.10	0.60	0.30	3.30	0.20	0.30	0.30
TOTAL	100.11	100.04	99.88	99.93	99.96	100.40	100.04	100.03	100.06	99.85	100.04	99.95	100.04

Explanatory notes: BDL = below detection limit, MgO < 0.10%, Na₂O < 0.1%, MnO < 0.1%, P₂O₅ < 0.01%

Table 2b:

Elements	SML-MR-1	SML-BS-1	SML-BS-2	SML-BS-3	SML-BS-4	SML-BS-5	SML-BS-6	SML-DS-1	SML-DS-2	SML-DS-3	SML-DS-4	SML-DS-5	SML-DS-6
Cl ppm	300	1500	400	800	400	400	1000	100	100	100	900	700	200
Sc ppm	BDL	BDL	BDL	BDL	BDL	20	BDL	14	24	BDL	24	14	36
V ppm	17	80	85	100	79	332	335	335	307	335	328	416	325
Cr ppm	9	76	64	86	32	277	200	320	295	260	288	322	214
Co ppm	1	21	21	14	11	225	164	49	135	184	129	107	186

Ni ppm	BDL	54	58	34	27	420	519	124	390	405	435	283	546
Cu ppm	11	29	26	13	26	801	466	7	58	264	18	179	221
Zn ppm	16	49	61	62	64	800	442	221	723	1161	445	279	892
Ga ppm	9	6	12	13.5	6	46	37	96	83	66	92	68	68
Ge ppm	1	1	0.7	0.7	1	1	0.7	1	1	0.7	1	1	1
As ppm	2	50.6	16	12	47	79	186	15	17	53	34	83	52
Se ppm	3	3	4	3	3	4	3	6	6	4	6	4	6.5
Br ppm	BDL	BDL	BDL	BDL	1	2	20	BDL	BDL	1	BDL	1	BDL
Rb ppm	2.9	18	45	46	23	130	192	49	18	153	37	158	16
Sr ppm	178	68	51	62	86	157	188	25	23	49	16	193	55
Y ppm	2	26	16	22	11	248	57	128	128	111	77	99.6	20
Zr ppm	12	35	75	54	37	235	210	440	457	464	486	436	17
Nb ppm	1	2	6	5.1	2	22	20	39	45	45	53	38	1
Mo ppm	1	11	8	5	3	37	49	3	3	20	1	29	14
Ag ppm	1	1	0.6	BDL	1	1	1	BDL	1	0.4	1	2	BDL
Cd ppm	BDL	2	0.6	0.5	BDL	5	4.5	3	4	1.2	3	2	1
Sn ppm	1	2	3	2	2	5	4	9	9	8	11	7	5
Sb ppm	16	7	2	3	3	16	27	4	6	6	7	14	3
Te ppm	1	1	0.6	2	1	8	1	1	BDL	0.8	2	1	2
I ppm	BDL	2	0.5	1	2	2	2	BDL	1	0.3	0.2	BDL	2
Cs ppm	4	6	6	7	5	10	16	3	3	10	3	9	4
Ba ppm	18	65	100	85	54	678	792	172	84	434	187	449	94
La ppm	7	33	26	26	18	198	143	325	170	140	193	152	67
Sm ppm	6	6.3	8.5	5	6	31	12	16	17	12	19	13	12
Ce ppm	10	30.5	46	30	32.5	384	212	207	338	156	354	210	66
Nd ppm	2	20	18	18	16	226	103	133	141	84	162	113.5	70
Yb ppm	BDL	BDL	BDL	BDL	BDL	BDL	BDL	BDL	BDL	BDL	BDL	BDL	BDL
Hf ppm	11	7	7	8	7	BDL	BDL	7	BDL	BDL	BDL	BDL	BDL

W ppm	29	30	30	24	26	40	18	48	40	34	61	16	19
Hg ppm	0.3	BDL	0.2	0.2	BDL	1	0.3	0.2	BDL	BDL	BDL	0.4	BDL
Tl ppm	1	4	4	3	1	12	58	26	38	16	26	18	56
Pb ppm	5	10	13	7	18	426	347	66	45	87	62.6	168	95
Bi ppm	BDL	BDL	BDL	BDL	BDL	5.5	BDL	BDL	BDL	3	BDL	BDL	BDL
Th ppm	0.4	2	3	BDL	21	27	10	24	34	26	39	20	BDL

Explanatory notes: BDL = below detection limit, Sc <10 ppm, Ni <10 ppm, Br <1 ppm, Ag < 0.3 ppm, Cd < 0.4 ppm, Te < 1 ppm, I < 1 ppm, Yb <1 ppm, Hf < 2 ppm, Hg <0.2 ppm, Bi <2 ppm, Th < 0.2 ppm

In Pearson's correlation coefficient system, Ga-Al₂O₃ is 0.985, Ga-Zr 0.864, and Zr-Al₂O₃ 0.890 (Figures 4-6). Similar positive correlations were calculated from the samples of the Parnassos-Oiti bauxites analyzed (Oikonomopoulou-Kyriakopoulou 1991), where Ga-Al₂O₃ is 0.613, Ga-Zr is 0.801, and Zr-Al₂O₃ is 0.711.

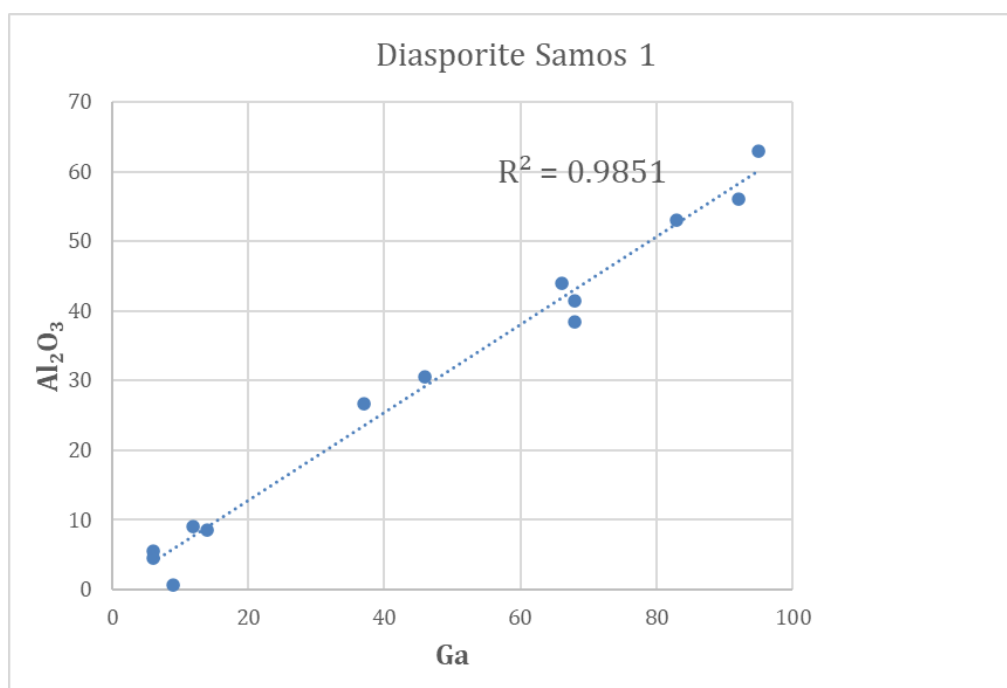


Fig. 4: Diagram showing the strong linear correlation observed in the Ga vs. Al₂O₃ scatterplot suggesting that gallium is structurally associated with the aluminum-bearing mineral phase diasporite in the Samos metabauxite. This is mineralogically significant because Ga³⁺ can substitute for Al³⁺ in the diasporite lattice due to their similar ionic radii and charges. The correlation implies that gallium is not present as a discrete mineral phase but is rather isomorphically incorporated into the crystal structure of diasporite.

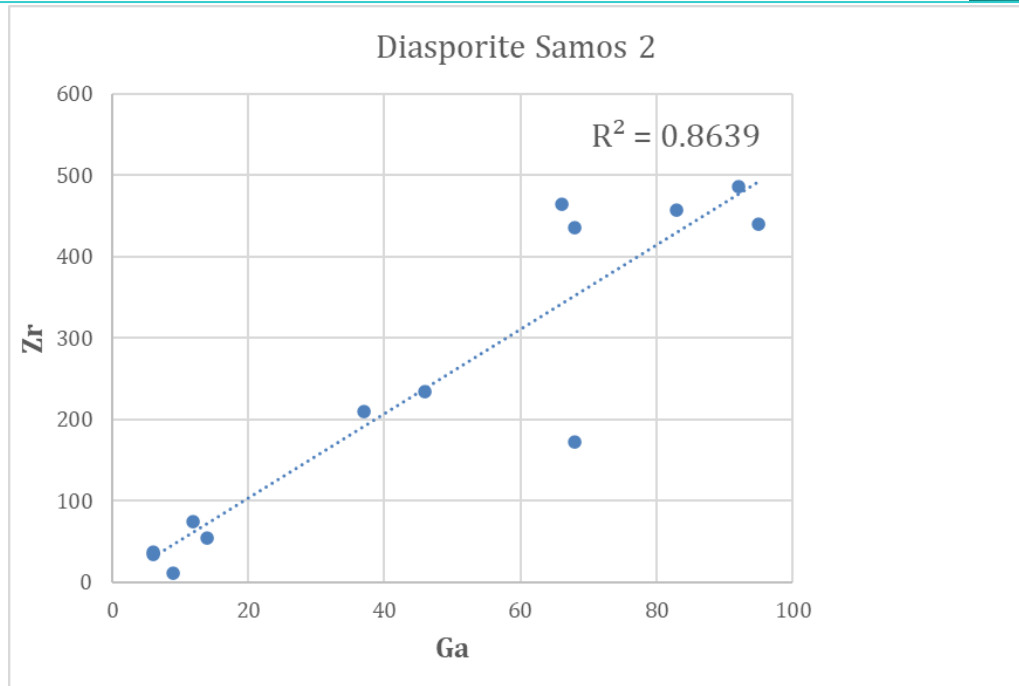


Fig. 5: X-Y scatterplot showing a linear, high correlation between Ga and Zr in diasporite from Samos Island, Greece. This observation indicates a likely mineralogical association between gallium and zirconium-bearing phases, most plausibly zircon ZrSiO_4 , as secondary zirconium-rich phases as those described from Brazilian bauxite deposits (Melfi et al. 1996) are absent. While Ga is primarily hosted in diasporite through isomorphic substitution for Al^{3+} , its correlation with Zr suggests that some gallium may also be associated with zircon grains present as accessory minerals. This could reflect co-precipitation or inclusion during diagenetic or metamorphic recrystallization processes.

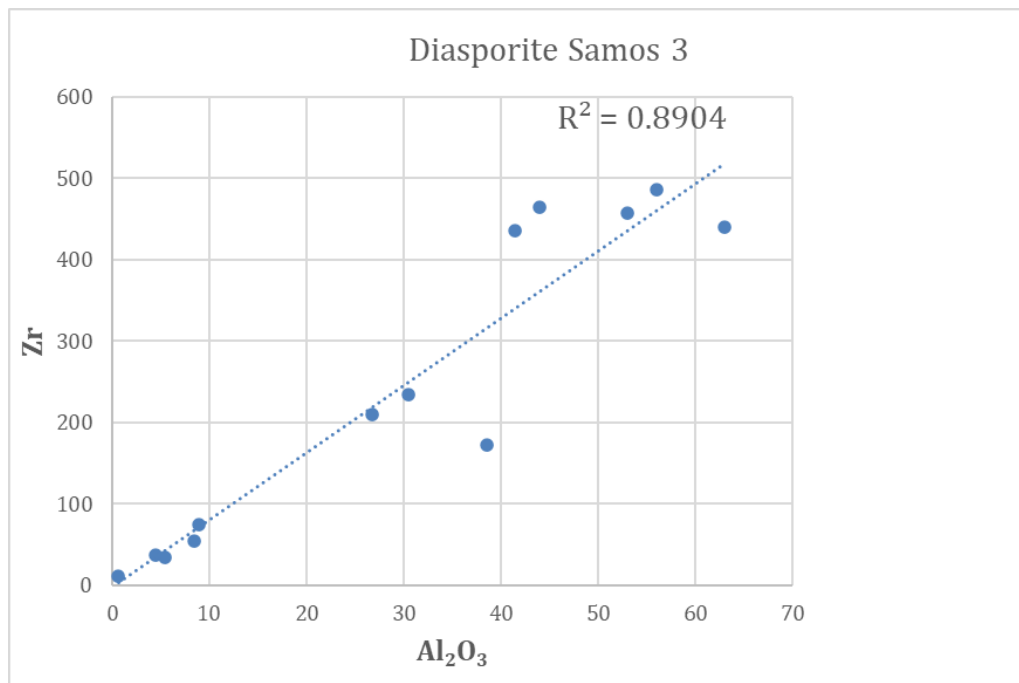


Fig. 6: Diagram showing the strong linear correlation between Al_2O_3 and Zr in the Samos diasporite, indicating that zircon ZrSiO_4 , though present in minor amounts, is enriched in aluminum-rich zones. This suggests that Zr was retained as a residual, refractory mineral during bauxitization and metamorphism, likely co-concentrating with diasporite. The correlation supports a textural or geochemical association between zircon and the aluminous phases in the metabauxite.

The group of Cr-Ni-Co has maximum concentrations 322-560-225 ppm respectively, values which are indicative for their derivation from basic rocks. Gabbro-type rocks occur north of Ireon village, whereas ultrabasic rocks occur close to Pagondas village, both included to the Ampelos Unit (Theodoropoulos 1979 a&b). The same group of elements in the bauxites of Parnassus-Ghiona have much higher concentrations of Cr-Ni, but not Co, reaching 1656-2100-56 ppm respectively (Oikonompoulou-Kyriakopoulou 1991). In the same group of bauxites Cr-Fe-bearing diasporite was detected (Gamaletsos et al. 2017), contrary to the chromium-bearing iron oxides/hydroxides which were detected in Mikri Lakka diasporite having 73.98% Fe_2O_3 , 4.62% Al_2O_3 , and 0.75% Cr.

The group of Pb-Zn-Mo has maximum concentrations 426-1161-49 ppm respectively, enrichments which could be attributed to the alteration of metamorphosed igneous rocks with acidic nature, like granitic gneiss which comprises part of the Menderes Massif (Bozkurt and Park 1994; Wiggins and Cemen 2023). Cu has also high values reaching 801ppm and it can be associated with both acid and basic igneous rocks. The unified group of Pb-Zn-Mo-Cu-Co could also be derived from an older than Late Neogene, weathered mineralization, as the well-studied epithermal sulphide deposits of the island of Samos, are associated with trachyte, rhyolite and syenite of Late Miocene age (Voudouris et al. 2019).

Under the SEM, there were detected fractured REE minerals, hosted in the aluminous ground mass (Plate 1). Ce, Y, Nd, La, Hf, Sm were detected by SEM and are present in the bulk XRF analysis. By contrast, Pr, Gd, Er, which were detected in the form of clastic grains by SEM, are not detectable in the bulk rock chemistry, due to the scarcity of their presence. Almost all REE detected are associated with the P_2O_5 , fixed together in the form of monazite (Plate 1a, and Stamatakis and Malegiannaki, 2018). However, as is shown in Plate 1, Zn, Cu, and As are also associated with some of the REE-rich minerals which are poor in phosphorus, or without phosphorus. It is therefore clear that, zinc and copper at least, occur in several forms in the deposit, as Feenstra (1997) has already been discovered the Zn/Al-rich minerals gahnite as well as zincohobomite, despite its occurrence in high-grade peraluminous metamorphites (Peteresen et al. 1989). In the marble, small quartz crystals, apatite and rutile were detected. Ga is also not detected by SEM as a gallium mineral, and it is most likely fixed in the lattice of diasporite replacing aluminum (Rudnik 2024). Well preserved zircon crystals were found, along with As, Zn, Pb and Cu compounds, especially in the porous earthy transition diasporite deposit. Zircon shows its typical chemical composition and only in

a few crystals the CaO and/or K₂O content is reaching 1%. There were not detected secondary Zr-rich phases as those occurring in several Brazilian bauxite deposits which are associated with Fe-rich and not Al-rich phases (Melfi et al. 1996; Duvallet et al. 1999; Balan et al. 2001).

Clastic grains of other metallic minerals are found during SEM-EDS analysis, disseminated in the diasporic groundmass (Plate 2). The main types detected are of the type: Fe₂O₃-Cu₂O (up to 1.63% Cu₂O), followed by BaO-PbO-SO₃, Fe₂O₃-Cu₂O-As₂O₃ (2.37% As₂O₃), Cu₂O-ZnO (58/39%). In several REE-rich grains, elevated values of ZnO-Cu₂O and CoO were also detected reaching up to 4.37-4.16 and 1.26% respectively. The Pb-rich REE mineral gramacciolite PbY (Ti, Fe)₂₀O₃₈ which was detected by Theye et al. (2010) was not detected during SEM-EDS analysis, probably due to its scarcity. Lead was only detected as oxide and/or sulphur minerals, along with barium (Table 2b, galena, anglesite, cerussite, and/or barite?).

5. Origin of trace element enrichments and derivation of alumina

According to Theodoropoulos' geological maps of Samos (1979 a&b), in the broad area of the NE Samos, the marbles of Zoodochos Pigi and the schists of Kotsikias-Psili Ammos are developed. Pre-Cenozoic basic, ultrabasic and acid igneous rocks occur in the central and western part of the island (Lowen et al. 2015). It is, therefore, plausible to assume a derivation of all trace elements enrichments and the source of alumina from the Mesozoic sediments (now meta-sediments) of the Ampelos Nape, present in Mikri Lakka, which include meta-sediments, meta-gabbros and meta-volcanics containing tourmaline, white mica, rutile, and zircon (Lowen et al. 2015). In addition, the adjacent Menderes Massif metamorphic rocks may have played an important role as source rocks. These rocks were weathered and altered under wet conditions releasing silica, alumina and iron, which formed diasporic deposits rest on a limestone (now marble) substrate. The significant differences of Ni, Cr and Co content of the bauxites of Central Greece and the East Samos reflects diverse parent rocks which were altered during Upper Cretaceous. Even between the three major bauxite horizons of Central Greece, there exist differences in trace element content, with the younger 3rd horizon, which is conformably overlaid by Upper Cretaceous limestones being much richer in Ni, V and Cr (Oikonomopoulou-Kyriakopoulou 1991).

The presence of euhedral zircon in the aluminous groundmass is common in bauxites, associated with other heavy minerals such as ilmenite and monazite, minerals that are also present in Mikri Lakka diasporite. The age of the zircons of the Ampelos Nape,

measured by Löwen et al. (2015), and Bröcker et al. (2014) varies, being Cambrian to Neoproterozoic in meta-sediments and Cretaceous in meta-gabbros. Zircon even though is a REE-bearing mineral, the Mikri Lakka zircons are solely composed of Zr oxide and silica, or contain small amounts of non-formula elements like calcium and potassium. Hay and Dempster (2009) suggest that the presence of euhedral zircon crystals in metamorphic rocks could represent feeding of the original basin from nearby volcanic centers. The same authors suggest that low temperature zircon formed during metamorphism may contain non-formula elements; hence the calcium and potassium-bearing zircons of Mikri Lakka may have similar origin. Richardson (1959) and Adams and Richardson (1960) studying several bauxite deposits of different origin pointed out that the highest concentration of zirconium was found in bauxites derived from acid igneous rocks having an average Zr content of 2480 ppm, whereas bauxites derived from basic igneous rocks have an average Zr content of 690 ppm, those derived from shales have average content of 590 ppm, and bauxites derived from carbonates contained the lowest concentrations of Zr with an average content of 480 ppm. However, Zainudeen et al (2023) have measured lower Zr content of some bauxite deposits derived from magnesium-ferrous andesite-basalt and mafic rocks, averaging 667 ppm and 414 ppm respectively. Oikonomopoulou-Kyriakopoulou (1991) has measured Zr content of the three horizons of the Mesozoic bauxite deposits of Central Greece, which have parent rocks basic and ultrabasic rocks, averaging 527 ppm. It is, therefore, important to consider some additional mineralogical and chemical parameters in order to identify the origin of the source rock, especially for the case that a series of alumina-rich rocks are present as precursor material.

Kelemen et al. (2023) suggest that besides the origin of bauxites from fluvial drainage of diverse metamorphic units, additional long-distance aeolian sources existed, related to igneous rocks. The zircon crystals studied from Löwen et al. (2015) extracted from Ampelos Nape rocks are mainly anhedral to subhedral, even though, some grains are recrystallised in two stages (Brocker et al. 2014). There is no indication that diasporite is a primary or secondary mineral formed during low grade metamorphism. The study of some Western Anatolian diasporite deposits from Milas area revealed that they are unique, as they contain both metamorphic and hydrothermal-remobilized diasporite, formed in different geological periods (Hatipoğlu et al., 2010a & 2010b).

It is known that in Cenomanian-Turonian succession of sediments, transgressive-regressive cycles have been reported in several Neo-Tethyan platforms, which are associated with hiatuses attributed to tectonic events and global sea-level fall (Lawa et al. 2023). Upper Turonian shallowing of the sea level was a significant event, having

been reported in carbonate successions in several places of Europe (Wiese and Kroger, 1998). During this shallowing of the sea-level, Upper Cretaceous, clastic grains of REE were transported into the sedimentary basin of East Samos, mainly with the form of monazite. Cu, Pb, Zn, As (and Co-Ni?) may represent weathered polymetallic deposit hosted in shales (now schists). Other trace elements present were probably fixed in the lattice of neoformed diaspore and other minerals. In particular, Ga^{3+} (0.62 nm) has similar ionic radius with Al^{3+} (0.57 nm), a fact that allows isomorphic substitutions in aluminum hydroxides such as diaspore (Foley et al. 2017; Ling et al. 2020).

The strong correlation of Zr with Al_2O_3 and Ga is also judging for a common, clastic origin of these elements in Samos diasporite. The parallel strong correlation of Zr, Ga, and Al_2O_3 of the Parnassus-Oiti bauxites, supports these genetic considerations. On the other hand, analysis of nine representative samples of Turkish bauxites and diaspore (Gündogan 2022) showed that there does not exhibit any correlation of Ga-Zr (-0.552) and Zr- Al_2O_3 (-0.738), and only Al_2O_3 -Ga shows a strong positive correlation (0.848). The variance of these correlations of Zr with both Al_2O_3 and Ga can be attributed to differences in the nature of the parent rocks which yield zircon, alumina and gallium in a sedimentary basin, as well as in percolating fluids chemistry and the degree of alteration. Bröcker and Pidgeon (2007) and Lowen et al. (2015) describe Triassic magmatic activity in several tectonic subunits of Cyclades. Even though there is no data describing pre-Cretaceous sulphide mineralization in Samos, SEM analysis, along with the trace element analysis judge for a possible derivation of Cu, Pb, Zn, Ba, Co, S, As, from altered sulphide primary mineralization.

6. Possible economic importance - Conclusions

According to a British Geological Survey report (Lusty et al. 2021), the Critical Metals with the highest Global Supply Risk are REE and Ga, along with Sb, Ge and Te, with the first two produced in China at 78% and 90% respectively. In China, where significant REE ore deposits occur, they are associated with peraluminous granites. This type of deposit is characterized as ion-adsorption deposit, formed by the subtropical weathering of granitoids, followed by the absorption of REEs as ionic complexes onto clay minerals (mostly kaolinite and halloysite) in the weathering crusts (Fan et al. 2023). Similar metallogenic systems are recently discovered in SE Asia, Madagascar and the southeastern United States (Xu et al. 2017). This type of deposits hosts almost 50% of the total mined HREE ore deposits worldwide (Boxleiter et al. 2024). Some peralkaline granites of Mongolia and Labrador, Canada are also rich in REE, whereas peraluminous granites of China, France, Egypt and Nigeria are poor in REE (Linnen and Cuney 2004).

Besides the granite-regolith associated REE deposits, kaolinite-rich sedimentary rocks and bauxite have a potential of hosting significant REE concentrations (Boxleiter et al. 2024). In Nova Scotia, Canada, the Late Devonian to Early Carboniferous Wentworth plutonic complex host mineralized zones which contain up to 3.4 wt% ZrO_2 , 1.2 wt% REE_2O_3 , and 0.4 wt% Nb_2O_5 (Ersay et al. 2022).

As it is shown in Table 2b, some of the HREE were not measured, or are absent from the bulk chemistry of the samples studied (Table 2b). One of the measured HREE is Yttrium, which has its higher concentration (248 ppm) in the transition deposits (BS). Ytterbium, even though it was detected by SEM-EDS analysis, is absent from the bulk rock chemistry. Scandium higher value was measured in the massive diasporite reaching 36ppm, whereas in half of the samples its content is below the detection limit. Neodymium is also enriched in the same massive diasporite sample reaching 226 ppm. The higher $\Sigma\text{REE}+\text{Y}$ content of Mikri Lakka massive diasporite is 1129 ppm, with an average value of 680 ppm, even though there had not been measured all REE. These values are much higher than the $\Sigma\text{REE}+\text{Y}$ measured in Parnassus-Ghiona bauxites which have an average content ranging between 292 ppm (Mondillo et al. 2022) and 463 ppm (Gamaletsos et al. 2019), the metabauxite deposits of Turkey which is 129 ppm (Gündogan 2022), and lower than the average $\Sigma\text{REE}+\text{Y}$ of the southern France karst-type Jurassic-Cretaceous bauxites which is 990.78 ppm. Mondillo et al. (2019) suggest that a recovery of REE has a potential interest due to the REEs release into solution, along with alumina and gallium, during the digestion step of the Bayer process.

Gallium is industrially produced as by-product during bauxite processing (>80%), and secondarily during processing of sediment-hosted Pb-Zn deposits (Schulte and Foley 2014; Qi et al. 2023; Critical Metals Corp. 2024). Gallium content of bauxites is of particular interest, as it can be extracted from the Al-ore during the Bayer process. Besides its importance as one of the critical metals in high-tech and green technology, Ga can be used as a diagnostic tool to study planetary evolution, surface weathering metallogenic systems and hydrothermal metallogenic systems, through its isotopes (Quin et al. 2025). Gallium in bauxites is enriched in the alumina hydroxide minerals whereas it is depleted in the accompanied in paragenesis iron hydroxides (Mondillo et al. 2019). The same authors have measured total Ga content up to 70.5 ppm in a series of bauxite samples, whereas Ga in the aluminum hydroxides is reaching the value of 178 ppm. In certain South American bauxite deposits gallium reaches up to 80 ppm of Ga_2O_3 (Critical Metals Corp. 2024). According to a USGS report (Schulte and Foley 2014), the range of gallium content of bauxites worldwide is ranging between ~10 to 812 ppm, with an average value of 57 ppm. More recent reports (Qi et al. 2023) separate

the Ga content of the karstic and lateritic bauxite worldwide, but they show almost the same average content, 59 ppm and 60 ppm respectively.

The Turkish bauxites contain in average 57 ppm Ga (26 representative samples analyzed; Hanilci 2019) and the meta-bauxites 51 ppm (8 representative samples; Gündoğan 2022). Note that in two average analyses of 100 (Oikonomopoulou-Kyriakopoulou 1991) and 22 (Mondillo et al. 2022) bauxite samples of the Greek Parnassus-Ghiona-Oiti deposits, gallium has slightly higher concentrations (64 and 67 ppm respectively), reaching up to 123 ppm in some unexploited bauxite occurrences (Oikonomopoulou-Kyriakopoulou 1991). These gallium average variances are common among bauxite deposits worldwide due to the variable samples used in each particular statistical analysis (Qi et al. 2023).

Liang et al (2023) have measured in muscovite derived from ore-related granite up to 139 pp gallium; the muscovite-rich samples of Mikri Lakka have not shown Ga enrichments, most likely due to their metamorphic origin. The average gallium content of the Mikri Lakka massive diasporite is 79 ppm (max 96 ppm), which is higher than the average gallium content of the exploiting Greek bauxite deposits and significantly higher than the cut-off grade of 20 ppm in bauxite ore deposits (Qi et al. 2023). Both the REE and Ga content of the Mikri Lakka diasporite is promising to consider their recovery from the ore, despite the fact that due to the absence of systematic borehole data, the proven reserves in the east part of Samos are unknown. These metals could be extracted as byproducts during the processing of the diasporite to produce alumina.

Acknowledgements

Thanks are expressed to TITAN SA laboratory staff of the Kamari Plant (Mrs. Katerina Issari and Mrs. Stella Tetsika), and the mining engineer of the company, Mr. Aimilios Georgiou for their valuable assistance and support during laboratory and fieldwork research. Thanks are also expressed to Mr. Vasileios Skounakis NKUA, for helping in SEM-EDS analysis. Finally, we owe to thank the anonymous referees for their valuable comments and suggestions.

References

Adams, J.A.S. and Richardson, K.A. 1960. Thorium, uranium and zirconium concentrations in bauxite. *Econ. Geol.*, V.55, p. 1653–1675. doi: <https://doi.org/10.2113/gsecongeo.55.8.1653>

Balan, E., Neuville, D.R., Trocellier, P., Fritsch, E., Muller, J.P. and Calas, G. 2001. Metamictization and chemical durability of detrital zircon *Amer. Mineral.*, V. 86, p. 1025-1033. <https://doi.org/10.2138/am-2001-8-909>

Bessenecker, H. and Buttner, D. 1978. Late Cenozoic sediments on the islands between Euboea and Turkey. In: H. Closs, D. Roeder, and K. Schmidt (Editors), *Alps, Apennines and Hellenides*. E. Schweizerbart'sche Verlagsbuch handlung, Stuttgart, pp. 502-506.

Boleti, A., 2014, Des outils simples en émeri dans le monde égéen. Une approche ethnoarchéologique. *Artefact* 2, 173-182. <https://doi.org/10.4000/artefact.9285>

Boxleiter, A., Wen, Y., Tang, Y., Elliott, W.C. 2024. Rare-earth element (REE) remobilization and fractionation in bauxite zones from sedimentary kaolin deposits, western Georgia (USA), Upper Coastal Plain, *Chemical Geology*, V. 660, 122151, ISSN 0009-2541, <https://doi.org/10.1016/j.chemgeo.2024.122151>

Bozkurt, E. and Park, L.R.G. 1994. Southern Menderes Massif: an incipient metamorphic core complex in western Anatolia, Turkey. *Jour. Geol. Soc.*, V. 151, p. 213-216. <https://doi.org/10.1144/gsjgs.151.2.0213>

Bröcker, M. and Pidgeon, R.T. 2007. Protolith Ages of Meta-igneous and Metatuffaceous Rocks from the Cycladic Blueschist Unit, Greece: Results of a Reconnaissance U-Pb Zircon Study. *Jour. Geology*, V. 117, p. 83-98.

Bröcker, M., Löwen, K., Rodionov, N. 2014. Unraveling protolith ages of meta-gabbros from Samos and the Attic–Cycladic Crystalline Belt, Greece: Results of a U–Pb zircon and Sr–Nd whole rock study, *Lithos*, V.198–199, p. 234-248, ISSN 0024-4937, <https://doi.org/10.1016/j.lithos.2014.03.029>

Calagari, A. and Abedini, A., 2007. Geochemical investigations on Permo-Triassic bauxite horizon at Kanisheeteh, east of Bukan, West-Azarbaidjan, Iran. *Journal of Geochemical Exploration*. V. 94, p. 1-18. <https://doi.org/10.1016/j.gexplo.2007.04.003>

Critical Metals Corp. 2024. Critical Metals Corp Discovers 147ppm of Gallium at its Tanbreez Project, Southern Greenland. November 2024, 2pp. <https://criticalmetalscorp.gcs-web.com/node/7246/pdf>

Dimou, E., Charalambidi, P., Epitropou, N, 2006. Mining activity in the island of Samos (in Greek). IGME, Athens, 115pp.

Duvallet, L., Martin, F., Soubies, F., Salvi, S., Melfi, A. J., Fortune, J. P. 1999. The mobility of zirconium and identification of secondary Zr-bearing phases in bauxite from Pocos de Caldas, Minas Gerais, Brazil; a mass-balance and X-ray absorption spectroscopic study. *Canad. Mineral.*, V. 37, p. 635-651.

Ersay, L., Greenough, J. D., Larson, K. P., & Dostal, J. 2022. Zircon reveals multistage, magmatic and hydrothermal Rare Earth Element mineralization at Debert Lake, Nova Scotia, Canada. *Ore Geology Reviews*, 144. [doi:10.1016/j.oregeorev.2022.104780](https://doi.org/10.1016/j.oregeorev.2022.104780)

Fan, Ch., Xu, Ch., Shi, A., Smith, M.P., Kynicky, J., Wei, Ch., 2023. Origin of heavy rare earth elements in highly fractionated peraluminous granites, *Geochimica et Cosmochimica Acta*, V. 343, p.371-383, ISSN 0016-7037, <https://doi.org/10.1016/j.gca.2022.12.019>

Feenstra, A., 1985. Metamorphism of bauxites on Naxos, Greece. Ph.D. Thesis, Rijksuniversiteit Utrecht, *Geologica Ultraiectina* V. 39, 206pp.

Feenstra, A., 1997. Zincohogbomite and gahnite in a diasporite-bearing metabauxite from eastern Samos (Greece): mineral chemistry, element partitioning and reaction relations. *Schweizerische Mineralogische und Petrographische Mitteilungen*, V. 77, p. 73– 93.

Feenstra, A., Urai, J., Wunder, B., 2001. The diasporite-corundite rock transformation in the Naxos metakarstbauxites: an example of dehydration-controlled weakening and recrystallisation. 13th Meeting on Deformation, Mechanisms, Rheology and Tectonics, Noordwijkerhout, the Netherlands. Book of abstracts, 1pp.

Foley, N.K., Jaskula, B.W., Kimball, B.E., and Schulte, R.F., 2017, Gallium, chap. H of Schulz, K.J., DeYoung, J.H., Jr., Seal, R.R., II, and Bradley, D.C., eds., *Critical mineral resources of the United States—Economic and environmental geology and prospects for future supply*: U.S. Geological Survey Professional Paper 1802, p. H1—H35, <https://doi.org/10.3133/pp1802H>

Gamaletsos, P.N., Godelitsas, A., Kasama, T., Church, N.S., Douvalis, A.P., Göttlicher, J., Steininger, R., Boubnov, A., Pontikes, Y., Tzamos, E., Bakas, T., Filippidis, A., 2017, Nano-mineralogy and -geochemistry of high-grade diasporic karst-type bauxite

from Parnassos-Ghiona mines, Greece, *Ore Geology Reviews*, V. 84, p.228-244, ISSN 0169-1368, <https://doi.org/10.1016/j.oregeorev.2016.11.009>

Gamaletsos, P.N., Godelitsas, A., Filippidis, A., and Pontikes Y. 2019. The Rare Earth Elements Potential of Greek Bauxite Active Mines in the Light of a Sustainable REE Demand. *J. Sustain. Metall.* V. 5, p. 20–47. <https://doi.org/10.1007/s40831-018-0192-2>

Ganas, A., Elias, P., Briole, P., Valkaniotis S., Escartin, J., Tsironi, V., Karasante I., Kosma Ch., 2021. Co-seismic and post-seismic deformation, field observations and fault model of the 30 October 2020 $M_w = 7.0$ Samos earthquake, Aegean Sea. *Acta Geophys.* V. 69, p. 999–1024. <https://doi.org/10.1007/s11600-021-00599-1>

Gessner, K., Ring, U., Güngör, T., 2011. Field Guide to Samos and the Menderes Massif: Along-Strike Variations in the Mediterranean Tethyan Orogen. The Geological Society of America Field Guide 23, 1-52. <https://doi.org/10.1130/9780813700236>

Gündoğan, I., 2022. Meta-bauxite deposit in the Tavşanlı Zone, NW Turkey: A new locality for gem-quality diaspore formation, *Jour. Asian Earth Sci.*: V. 8, 20pp., 100114, <https://doi.org/10.1016/j.jaesx.2022.100114>

Hanilci, N. 2029. Bauxite deposits of Turkey. In: F. Piranjo et al. eds., *Mineral Resources of Turkey, Modern approaches*, in *Solid Earth Sciences*, Chapter 15, p. 681-730, Springer Nature. https://doi.org/10.1007/978-3-030-02950-0_15

Hatipoğlu, M., Helvacı, C., Chamberlain, S. C., Babalik, H., 2010a. Mineralogical characteristics of unusual “Anatolian” diaspore (zultanite) crystals from the İlbirdağı diasporite deposit, Turkey. *Journal of African Earth Sciences* V. 57, p. 525-541. <https://doi.org/10.1016/j.jafrearsci.2010.01.002>

Hatipoğlu, M., Türk, N., Chamberlain, S. C., Akgün, A. M., 2010b. Metabauxite horizons containing remobilized-origin gem diaspore and related mineralization, Milas-Muğla province, SW Turkey. *Journal of Asian Earth Sciences* V. 39, p. 359-370. <https://doi.org/10.1016/j.jseaes.2010.04.016>

Hay, D. and Dempster, T. 2009. Zircon Behaviour during Low-temperature Metamorphism. *Journal of Petrology*, V. 50, p. 571-589, <https://doi.org/10.1093/petrology/egp011>

Kelemen, P., Dunkl, I., Csillag, G. [Mindszenty A.](#), [Józsa S.](#), [Fodor L.](#), [von Eynatten H.](#) 2023. Origin, timing and paleogeographic implications of Paleogene karst bauxites in the northern Transdanubian range, Hungary. *Int J Earth Sci (Geol Rundsch)* 112, 243–264. <https://doi.org/10.1007/s00531-022-02249-3>

Lapparent, J. De., 1937. L' emeri de Samos. Mineralogische und Petrographische Mitteilungen (Tschermarks), V. 49, p.1-30.

Lawa, F.A., Mohammed, I., Farouk S., Ahmad F., Faris, M., Tanner, L., Al-Kahtany, K., 2023. Stratigraphic architecture of the Tethyan Cenomanian-Turonian succession and OAE2 in the Dokan Area, Kurdistan Region, northeast Iraq, *Journal of African Earth Sciences*, 207, 17 pp., 105064, <https://doi.org/10.1016/j.jafrearsci.2023.105064>

Liang, W., Ren, T., Guan, S., Yi, Y., Zhang, D., Yang, T., Luo, X., Huang, J., Zhang, Q., Bao, G. 2023. Gallium distribution in the Dulong Sn polymetallic deposit, SW China, *Ore Geology Reviews*, 163, 105821, <https://doi.org/10.1016/j.oregeorev.2023.105821>

Ling, K.Y., Tang, H.S., Zhang, Z.W., Wen, H.J. 2020. Host minerals of Li–Ga–V–rare earth elements in Carboniferous karstic bauxites in southwest China, *Ore Geology Reviews*, 119, 13 pp., 103325, <https://doi.org/10.1016/j.oregeorev.2020.103325>

Linnen, R.L. and Cuney, M. 2004. Grannite-related rare element deposits and experimental constraints on Ta-Nb-W-Sn-Zr-Hf mineralization. In: *Rare-element geochemistry and mineral deposits*, Linnen R.L. and Samson I.M. Editors, GAC Short Course Notes 17, p. 45-68, Ontario, Canada.

Löwen, K., Bröcker, M. Berndt, J. 2015. Depositional ages of clastic metasediments from Samos and Syros, Greece: results of a detrital zircon study. *International Journal of Earth Sciences*, 104, p. 205-220, <https://doi.org/10.1007/s00531-014-1058-x>

Lusty, P.A.J., Shaw, R.A., Gunn, A.G., Idoine, N.E. 2021. UK critical assessment of technology critical minerals and metals. British Geological Survey Commissioned Report CR/21/120, 76pp.

Melfi, A. J., Subies, F., Nahon, D., Formoso, M.L.L. 1996. Zirconium mobility in bauxites of Southern Brazil. *Jour. South Amer. Earth Sci.*, V. 9, p. 161-170, ISSN 0895-9811, [https://doi.org/10.1016/0895-9811\(96\)00003-X](https://doi.org/10.1016/0895-9811(96)00003-X)

Mondillo, N., Balassone, G., Boni, M., Chelle-Michou, C., Cretella, S., Mormone, A., Putzolu, F., Santoro, L., Scognamiglio, G., and Tarallo, M. 2019. Rare Earth Elements (REE) in Al- and Fe-(Oxy)-Hydroxides in Bauxites of Provence and Languedoc (Southern France): Implications for the Potential Recovery of REEs as By-Products of Bauxite Mining, *Minerals*, V. 9, p. 504-522, <https://doi.org/10.3390/min9090504>

Mondillo, N. Di Nuzzo, M., Kalaitzidis, S., Boni, M., Santoro, L., Balassone, G., 2022. Petrographic and geochemical features of the B3 bauxite horizon (Cenomanian-Turonian) in the Parnassos-Ghiona area: A contribution towards the genesis of the Greek karst bauxites, *Ore Geology Reviews*, 143, 16pp., 104759, ISSN 0169-1368, <https://doi.org/10.1016/j.oregeorev.2022.104759>

Mordberg, L.E., 1993. Patterns of distribution and behaviour of trace elements in bauxites, *Chemical Geology*, 107, Issues 3–4, p. 241-244, ISSN 0009-2541, [https://doi.org/10.1016/0009-2541\(93\)90183-J](https://doi.org/10.1016/0009-2541(93)90183-J)

Mposkos, E., 1986. The metamorphic basement of Samos: evidences indicating the type and grade of metamorphism. *Bull. Geol. Soc. Greece*, 18, p. 223-236.

Oikonomopoulou-Kyriakopoulou, N. 1991. A comparative geochemical and mineralogical study of the bauxite horizons of Central Greece. PhD Thesis, NTUA, Athens, 119pp.

Papanikolaou, D. 1979. Unités tectoniques et phases de déformation dans l'île de Samos, Mer Egée, Grèce. *Bulletin de la Société Géologique de France* 7, 21, 745-752. <https://doi.org/10.2113/gssgfbull.S7-XXI.6.745>

Papanikolaou, D. 2021. *The Geology of Greece*. Springer, 393pp, ISBN 10: 3030607305, and ISBN 13: 9783030607302

Petersen, E.U., Essene, E.J., Peacor, D.R., Marcotty L.A. 1989. The occurrence of hōgbomite in high-grade metamorphic rocks. *Contr. Mineral. Petrol.* 101, p. 350–360. <https://doi.org/10.1007/BF00375319>

Qi, H., Gong, N., Zhang S. Q., Li, J., Yuan, G. L., Liu, X. F. 2023. Research progress on the enrichment of gallium in bauxite, *Ore Geology Reviews*, 160, 9pp., 105609, ISSN 0169-1368, <https://doi.org/10.1016/j.oregeorev.2023.105609>

Richardson, K.A. 1959. The thorium, uranium and zirconium concentration in bauxites and their relationship in bauxite genesis. MSci. Thesis, The Rice Institute Library, Huston, Texas USA, 63pp.

Ring, U., Laws, S., Bernet, M. 1999: Structural analysis of a complex nape sequence and late-orogenic basins from the Aegean Island of Samos, Greece. *Journal of Structural Geology*, 21/11, p. 1575-1601, ISSN 0191-8141, [https://doi.org/10.1016/S0191-814\(99\)00108-X](https://doi.org/10.1016/S0191-814(99)00108-X)

Ring, U., Okrusch, M., Will T. 2007. Samos Island, part I: metamorphosed and non-metamorphosed nappes, and sedimentary basins. *J Virt. Explor.*, 27, p.1–28.

Rudnik, E. 2024. Review on Gallium in Coal and Coal Waste Materials: Exploring Strategies for Hydrometallurgical Metal Recovery. *Molecules*, 29, 40pp, <https://doi.org/10.3390/molecules29245919>

Saber, S.G., Salama, Y.F., Scott, R.W., Abdel-Gawad, G.I., Aly M.F. 2009. Cenomanian-Turonian rudist assemblages and sequence stratigraphy on the North Sinai carbonate shelf, Egypt. *GeoArabia*, 14, p. 113–134. doi: <https://doi.org/10.2113/geoarabia1404113>

Schulte, R.F. and Foley, N.K. 2014. Compilation of Gallium resource data for bauxite deposits. Mineral Resources Program, Open-File Report 2013-1272, USGS, Reston, Virginia, 14 pp. ISSN 2331-1258, <http://dx.doi.org/10.3133/ofr20131272/>

Stamatakis, M., 1986. Boron distribution in hot springs, volcanic emanations, marine evaporites and in volcanic and sedimentary rocks of Cenozoic age in Greece. Ph.D. Thesis, National and Kapodistrian University of Athens, Athens, 495 pp.

Stamatakis, M., & Malegiannaki, I. A. 2018. The exploitation of emery on the island of Samos: Existing data and research perspectives. *Bulletin of the Geological Society of Greece*, V. 53, p. 1–27. <https://doi.org/10.12681/bgsg.18575>

Theodoropoulos, D. 1979a. Samos Island, geological map 1:50,000, Vathy sheet, with explanations. Institute of Geological Mining Research, Athens, Greece.

Theodoropoulos, D. 1979b. Samos Island, geological map 1:50,000, Karlovassi sheet, with explanations. Institute of Geological Mining Research, Athens, Greece.

Theye, T., Hatert, F., Ockenga, E., Bertoldi, C., Lathe, C., 2010. Gramaccioliite(Y): paragenesis chemistry, and structure in a new occurrence, Samos Island, Greece. *Eur. J. Mineral* 22, 443–452. <https://doi.org/10.1127/0935-1221/2010/0022-2020>

Urai, J. L., Feenstra, A., 2001. Weakening associated with the diaspore-corundum dehydration reaction in metabauxites: an example from Naxos (Greece). *Journal of Structural Geology* 23, 941-950, [https://doi.org/10.1016/S0191-8141\(00\)00165-6](https://doi.org/10.1016/S0191-8141(00)00165-6)

U.S. Geological Survey, 2021. Mineral commodity summaries 2021: U.S. Geological Survey, 200 p., <https://doi.org/10.3133/mcs2021>

Villanova-de-Benavent, C., Proenza, J.A., Torró, L., Aiglsperger, Th., Domènech C., Domínguez-Carretero D., Llovet X., Suñer P., Ramírez A., Rodríguez J. 2023. REE ultra-rich karst bauxite deposits in the Pedernales Peninsula, Dominican Republic: Mineralogy of REE phosphates and carbonates, *Ore Geology Reviews*, Volume 157, 105422, ISSN 0169-1368, <https://doi.org/10.1016/j.oregeorev.2023.105422>

Voudouris, P., Mavrogonatos, C., Spry, P.G., Baker, T., Melfos, V., Klemd, R., Haase, K., Repstock, A., Djiba, A., Bismayer U., Tarantola A., Scheffer C., Moritz R., Kouzmanov K., Alfieris D., Papavassiliou K., Schaarschmidt A., Galanopoulos E., Galanos E., Kołodziejczyk J., Stergiou C., Melfou M. 2019. Porphyry and epithermal deposits in Greece: An overview, new discoveries, and mineralogical constraints on their genesis, *Ore Geology Reviews*, V 107, p. 654-691, ISSN 0169-1368, <https://doi.org/10.1016/j.oregeorev.2019.03.019>

Weidmann, M., Solounias, N., Drake R.E., Curtis J. 1984. Neogene stratigraphy of the Mytilini Basin, Samos Island, Greece. *Geobios* V. 17, p. 477–490.

Wiese, F. and Kröger, B. 1998. Evidence for a shallowing event in the Upper Turonian (Cretaceous) *Mytiloides scupini* Zone of northern Germany. *Acta Geologica Polonica*, V. 48, p. 265-284.

Wiggins, A., and Çemen, İ. 2023. Geothermal gradient variation in the Büyük Menderes Graben: implications for geothermal potential of the graben. *Bull. Miner. Res. and Explor.* V. 171, p. 123-142. <https://doi.org/10.19111/bulletinofmre.1293039>

Xu,, Ch., Kynický, J., Smith, M.P., Kopriva, A., Brtnicky, M., Urubek, T.,Yang Y., Zhao Z., He Ch., Song W. 2017. Origin of heavy rare earth mineralization in South China. Nat. Commun. V. 8, 14598. <https://doi.org/10.1038/ncomms14598>

Zainudeen, N.M., Mohammed, L., Nyamful, A., Adotey, D., Osae S.K., 2023. A comparative review of the mineralogical and chemical composition of African major bauxite deposits. Heliyon, V. 12, 22pp. <https://doi.org/10.1016/j.heliyon.2023.e19070>

Zemeyi, L. 2025. Altona uncovers high-grade gallium mineralization at Monte Muambe Project. Mozambique Mining Journal, 1pp, April 18th 2025.

APPENDIX

Plate 1: SEM-EDS analysis. The distribution of REE-rich minerals (white) in a diasporite/titanomagnetite groundmass (dark). a) P, Y, Gd, Er-rich -monazite, b) Cu-As, Ce, La, Pr, Nd-rich, c) Ca, La, Ce, Pr, Nd, Sm-rich, d) Zn, Ce, Pr, Nd, Sm-rich.

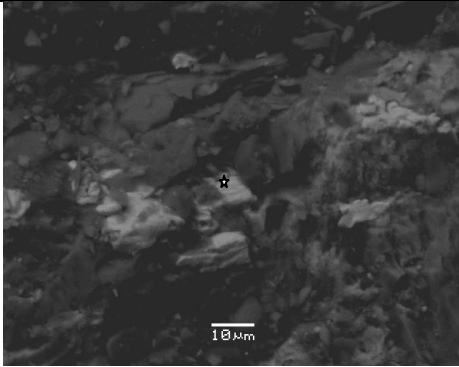
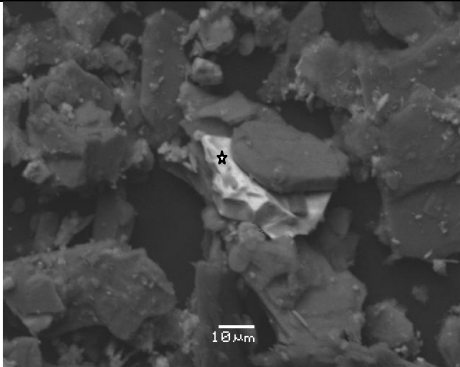
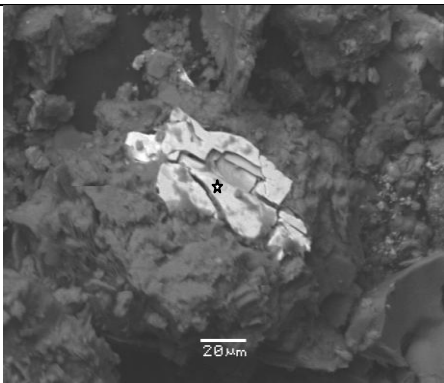
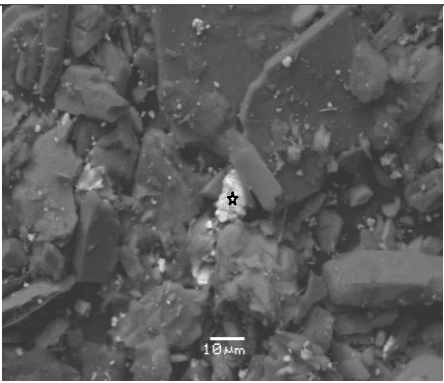
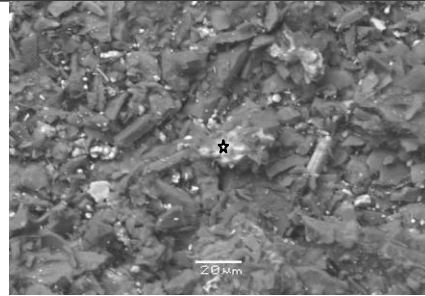
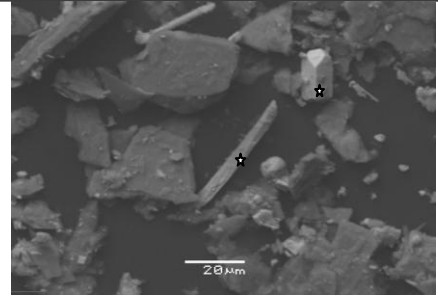
 <p>a) SML-DS-2: SiO₂ 12.81%, P₂O₅ 27.10%, K₂O 0.81%, CaO 1.33%, Fe₂O₃ 5.85%, Y₂O₃ 32.24%, Gd₂O₃ 1.67%, Er₂O₃ 1.33%</p>	 <p>b) SML-BS-4: Al₂O₃ 6.43%, SiO₂ 5.40%, P₂O₅ 5.00%, K₂O 0.68%, Fe₂O₃ 1.18%, Cu₂O 1.19%, As₂O₃ 0.64%, La₂O₃ 16.25%, CeO₂ 25.87%, Pr₂O₃ 4.15%, Nd₂O₃ 11.59%, ThO₂ 1.16%</p>
 <p>c) SML-DS-6: Al₂O₃ 4.57%, SiO₂ 4.10%, CaO 11.35%, Fe₂O₃ 0.74%, La₂O₃ 21.80%, CeO₂ 25.98%, Pr₂O₃ 3.16%, Nd₂O₃ 12.34%, Sm₂O₃ 2.23%</p>	 <p>d) SML-BS-6: Al₂O₃ 10.10%, SiO₂ 7.28%, K₂O 1.11%, Fe₂O₃ 3.31%, ZnO 2.51%, CeO₂ 30.83%, Pr₂O₃ 2.94%, Nd₂O₃ 9.23%, Sm₂O₃ 1.95%, ThO₂ 1.29%</p>

Plate 2: SEM-EDS analysis. Subhedral diasporic elongated crystals hosting scattered iron oxides (85.20%), rich in Cu_2O (1.62%) [a]. Euhedral zircon prism (upper right) which and broken rutile needle-like crystal (center) [b].



a] SML-DS-1



b] SML-DS-1